2023-07-14

Constrained tropical land temperature-precipitation sensitivity reveals decreasing evapotranspiration and faster vegetation greening in CMIP6 projections

Zhu, B

10.1038/s41612-023-00419-x
npj Climate and Atmospheric Science
Springer Science and Business Media LLC

SUPPORTING INFORMATION FOR:

Constrained tropical land temperature-precipitation sensitivity reveals decreasing evapotranspiration and faster vegetation greening in CMIP6 projections

Authors: Boyuan Zhu[1,2], Yongzhou Cheng[1,2], Xuyue Hu[1,2], Yuanfang Chai[3✉], Wouter R. Berghuijs[4], Alistair G. L. Borthwick[5,6], Louise Slater[7].

Affiliations:

1 School of Hydraulic and Environmental Engineering, Changsha University of Science & Technology, Changsha 410114, China

2 Key Laboratory of Water-Sediment Sciences and Water Disaster Prevention of Hunan Province, Changsha 410114, China

3 State Key Laboratory of Earth Surface Processes and Resource Ecology, Faculty of Geographical Science, Beijing Normal University, Beijing 100875, China.

4 Department of Earth Sciences, Free University Amsterdam, Amsterdam 1081 HV, the Netherlands

5 School of Engineering, The University of Edinburgh, Edinburgh EH9 3JL, UK

6 School of Engineering, Computing and Mathematics, University of Plymouth, Plymouth PL4 8AA, UK

7 School of Geography and the Environment, University of Oxford, Oxford OX1 3QY, UK

email: yuanfangchai@163.com

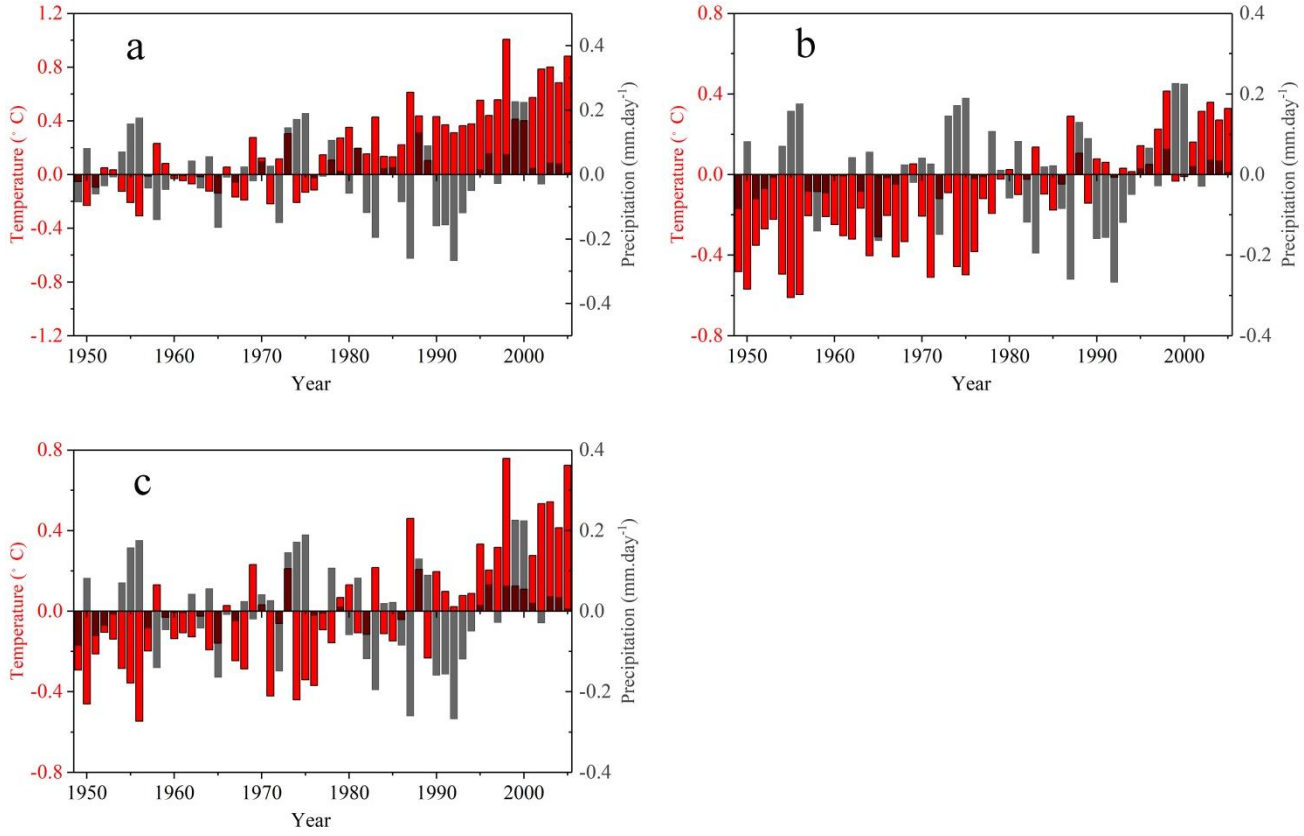

Supplementary Fig. 1 Observed time series of annual land-surface temperature and precipitation in the tropical zone for three other datasets: a, GISS+GPCC, **b,** NOAA+GPCC, and **c,** Delaware.

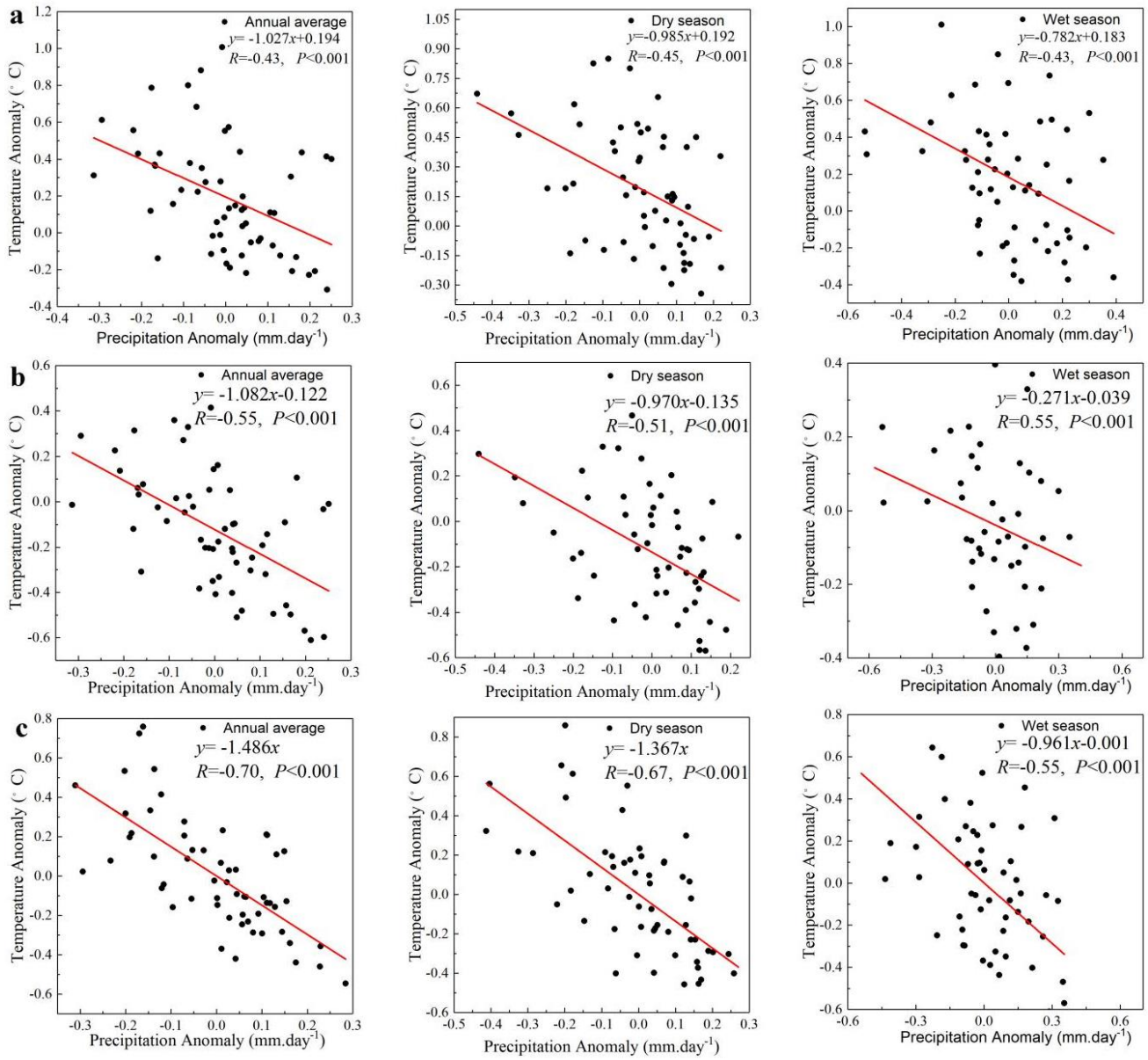

Supplementary Fig. 2 Annual and seasonal linear regressions between tropical land-surface temperature and precipitation anomalies based on observed data from three other datasets. a, GISS+GPCC, **b,** NOAA+GPCC, and **c,** Delaware.

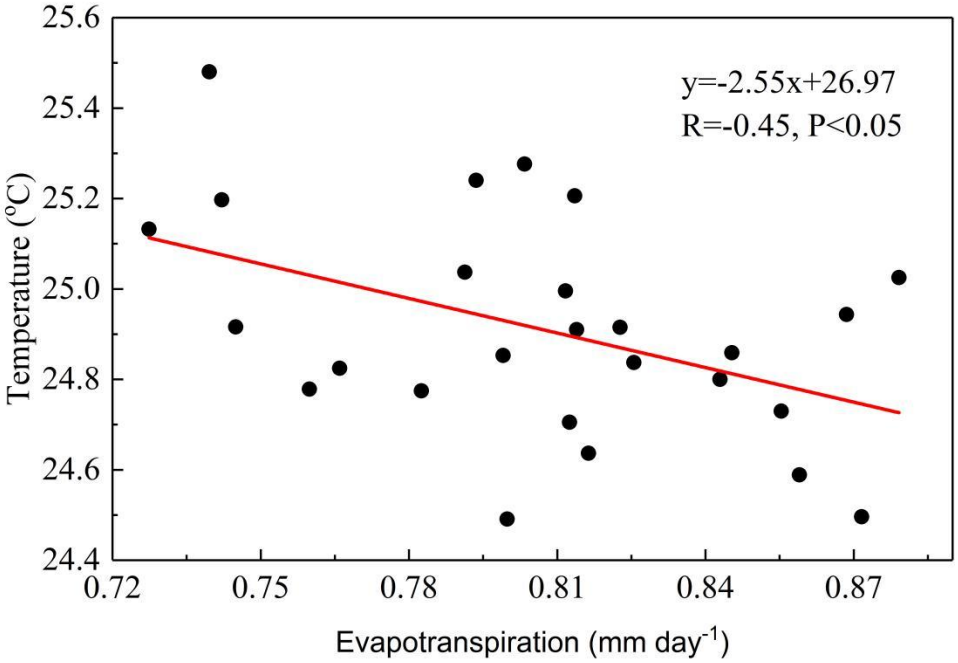

Supplementary Fig. 3 Relationship between observations of tropical land-surface evapotranspiration from the GLEAM dataset and temperature from the HadCRUT4 dataset during 1980-2005.

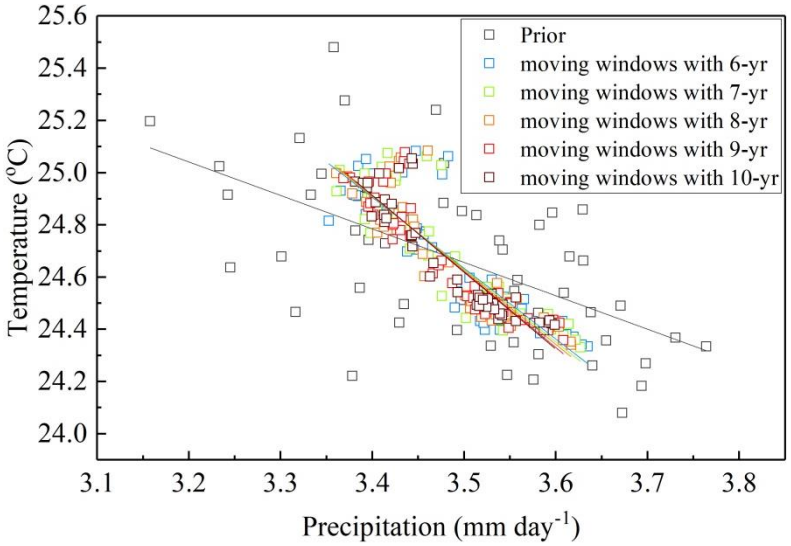

Supplementary Fig. 4 Linear relationships between observed tropical land-surface temperature and precipitation before and after using a moving average with window lengths ranging from 6 to 10 years.

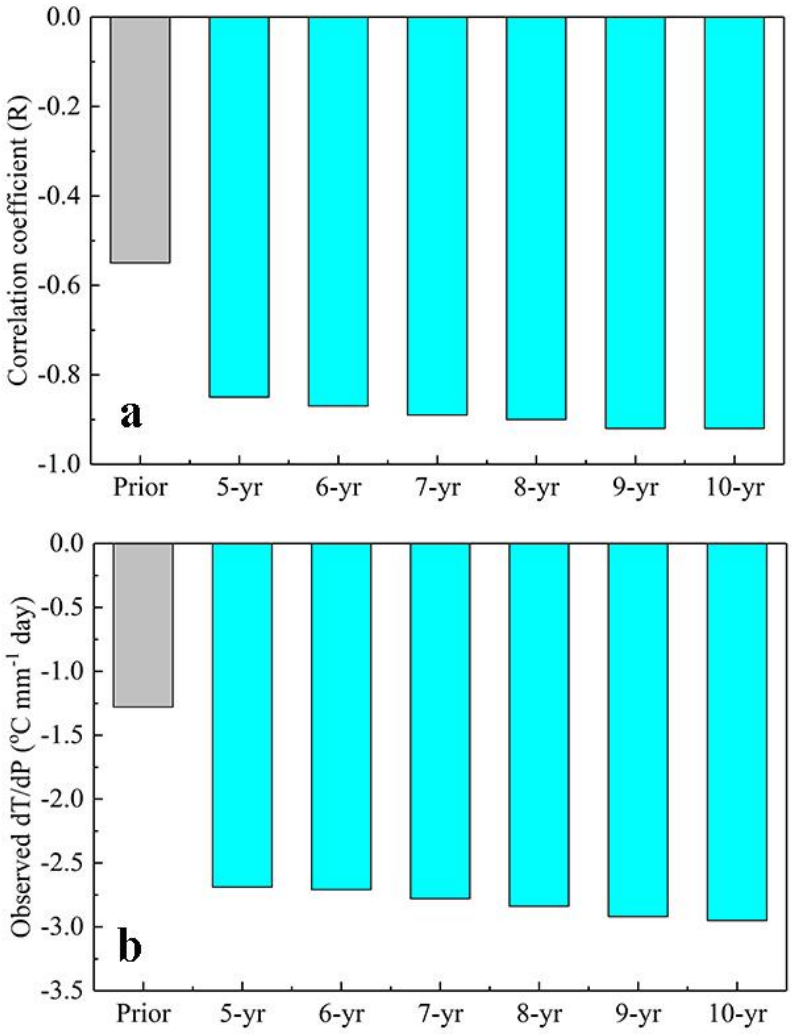

Supplementary Fig. 5 Correlation and slope from linear regressions between observed tropical land-surface temperature and precipitation before and after using moving averages with different window lengths (from 5 to 10 years). a, Correlation coefficients of the regressions. **b,** Observed d*T*/d*P* values obtained from slopes of the regressions. Note: the linear regressions are provided in Fig.1d in the Main Text.

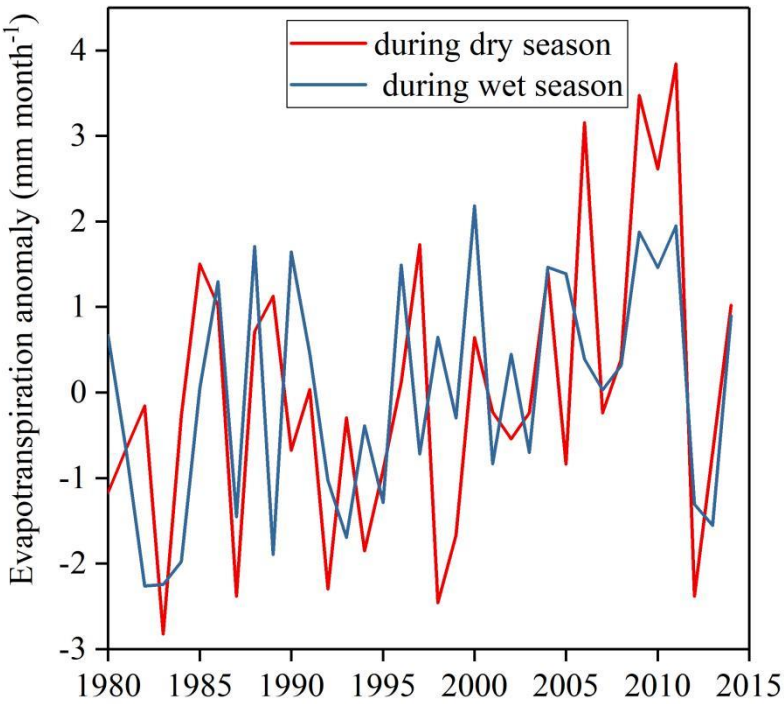

Supplementary Fig. 6 Observed yearly evapotranspiration anomaly from 1980 to 2014. The anomaly in this plot is computed as the value of evapotranspiration in a certain year minus the mean over the multi-year period of 1980-2014.

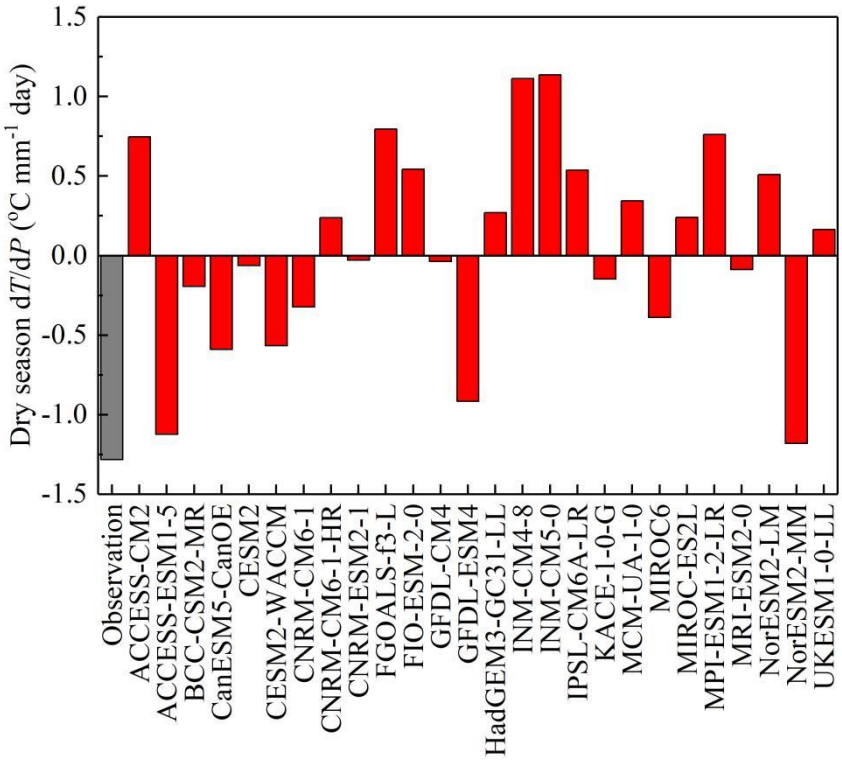

Supplementary Fig. 7 Observed historical dry-season d*T*/d*P* from the HadCRUT4 dataset and simulated values from the 26 CMIP6 models for temperature/precipitation in Supplementary Table 1.

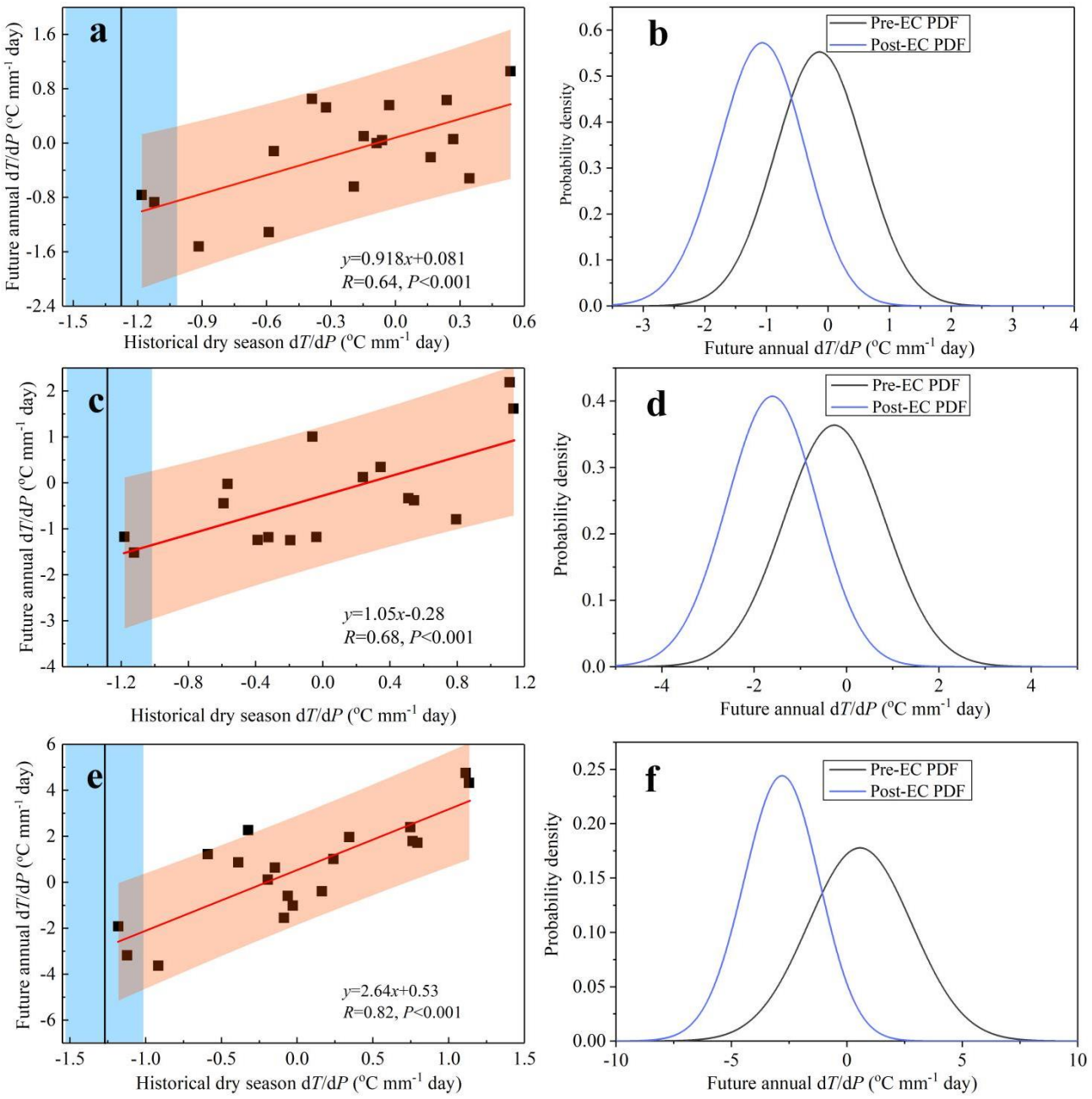

Supplementary Fig. 8 ECs on future annual d*T*/d*P* based on CMIP6 models under the other three SSP scenarios. a, **c** and **e,** The emergent relationships for SSP126, SSP245, and SSP370 scenarios, respectively. The constraint consists of a linear regression (with the associated forecast error) between the future annual simulated d*T*/d*P* and the historical dry season simulated d*T*/d*P* (red line and orange shaded area); then the constrained data is computed by projecting the observed historical dry season d*T*/d*P* ± one standard deviation (vertical black line and light blue rectangle, obtained from the HadCRUT4 dataset) onto the regression. **b**, **d** and **f,** PDFs for SSP126, SSP245, and SSP370 scenarios, respectively. Blue and grey lines are PDFs for the constrained (post-EC) and unconstrained (Pre-EC) future annual d*T*/d*P*, showing the change in forecast uncertainty and the best estimate of future annual d*T*/d*P*.

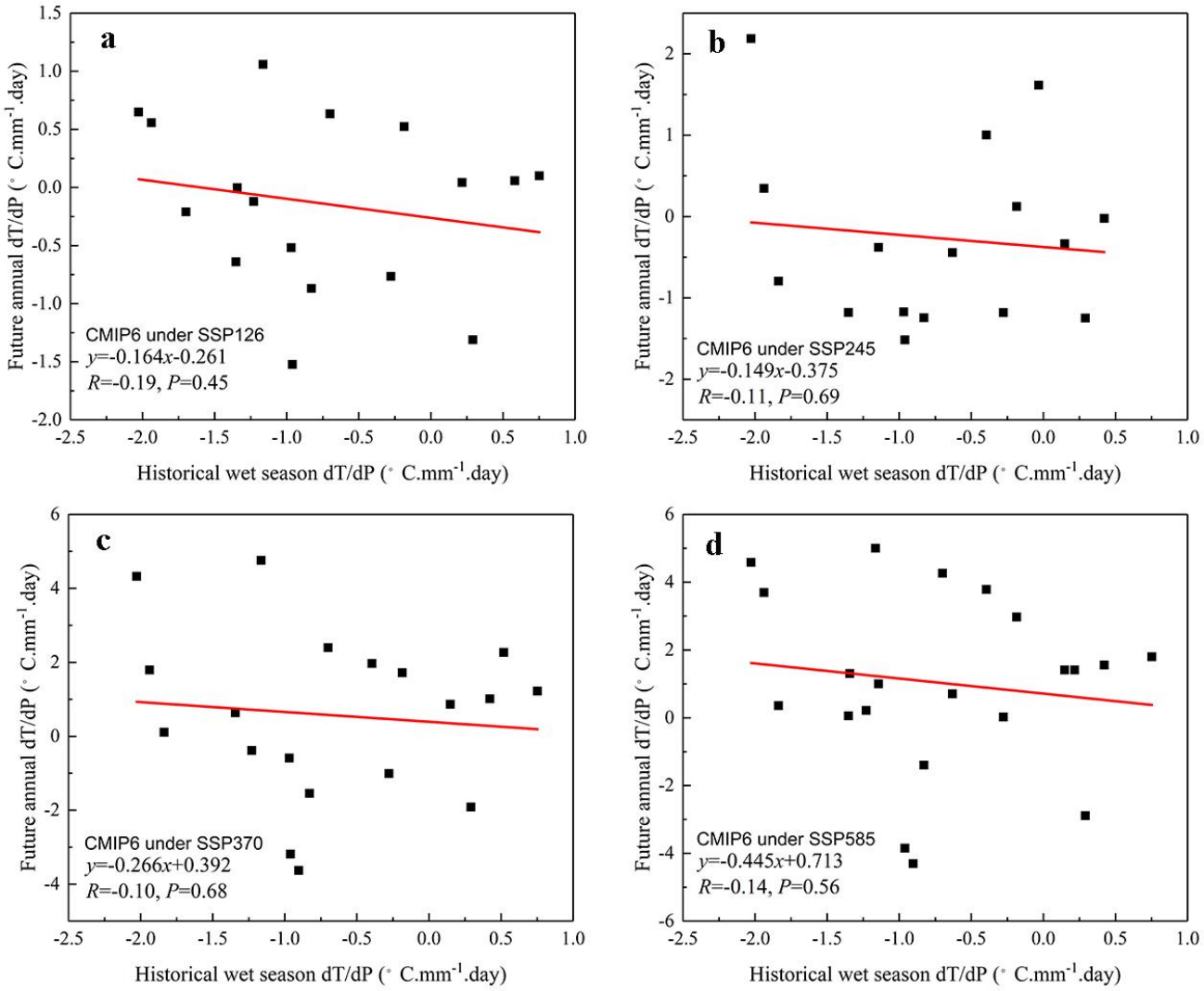

Supplementary Fig. 9 Relationship between future annual and historical wet season values of tropical land-surface d*T*/d*P* derived from CMIP6 models under the four SSP scenarios: a, SSP126, **b,** SSP245, **c,** SSP370, and **d,** SSP585.

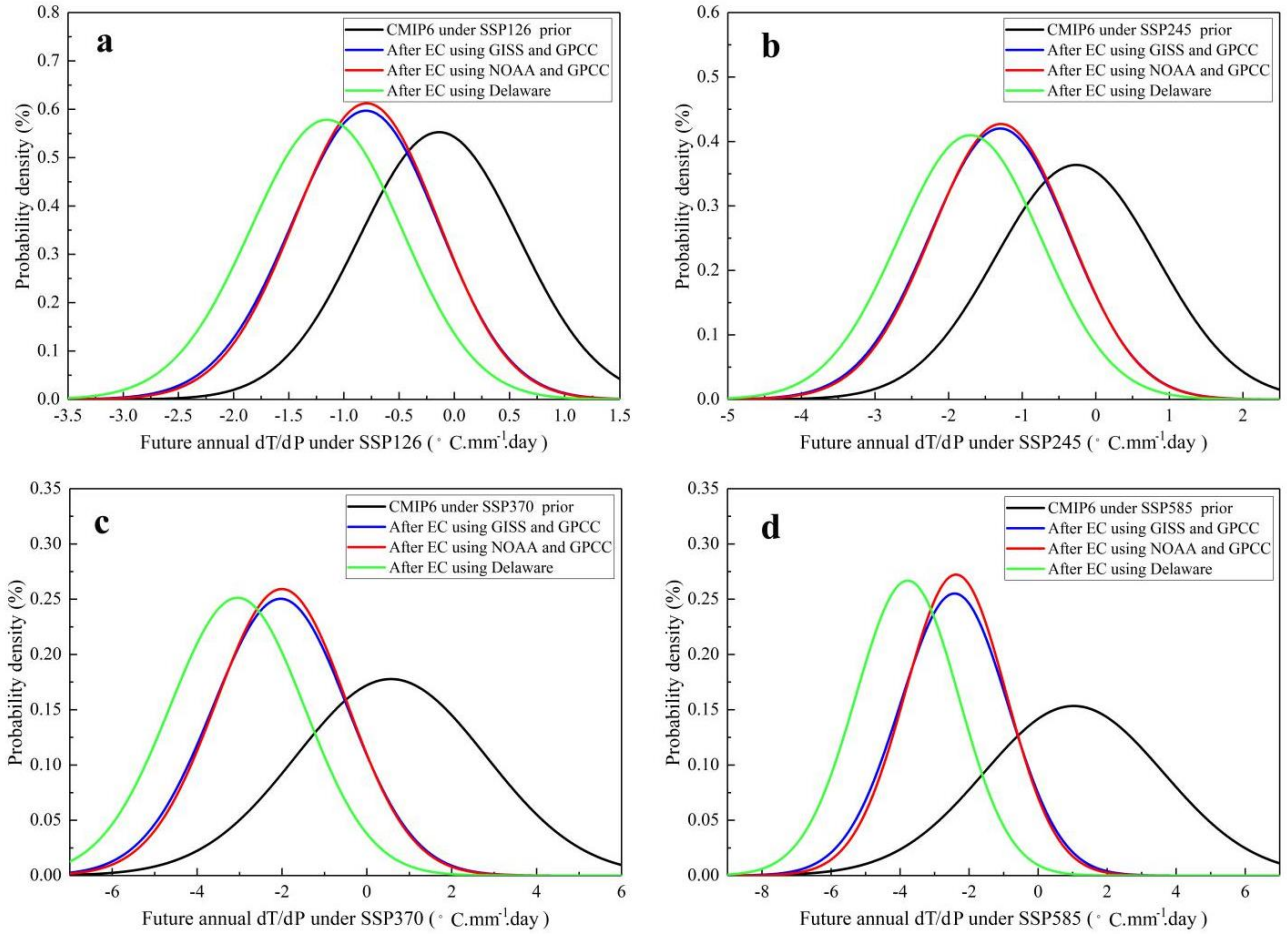

Supplementary Fig. 10 Pre-EC and post-EC PDFs for future annual tropical land-surface d*T*/d*P* based on CMIP6 models, in which the post-EC results are based on the GISS+GPCC, GPCC+NOAA, and Delaware datasets. These PDFs are respectively deduced from **a,** the SSP126 scenario, **b,** the SSP245 scenario, **c,** the SSP370 scenario, and **d,** the SSP585 scenario.

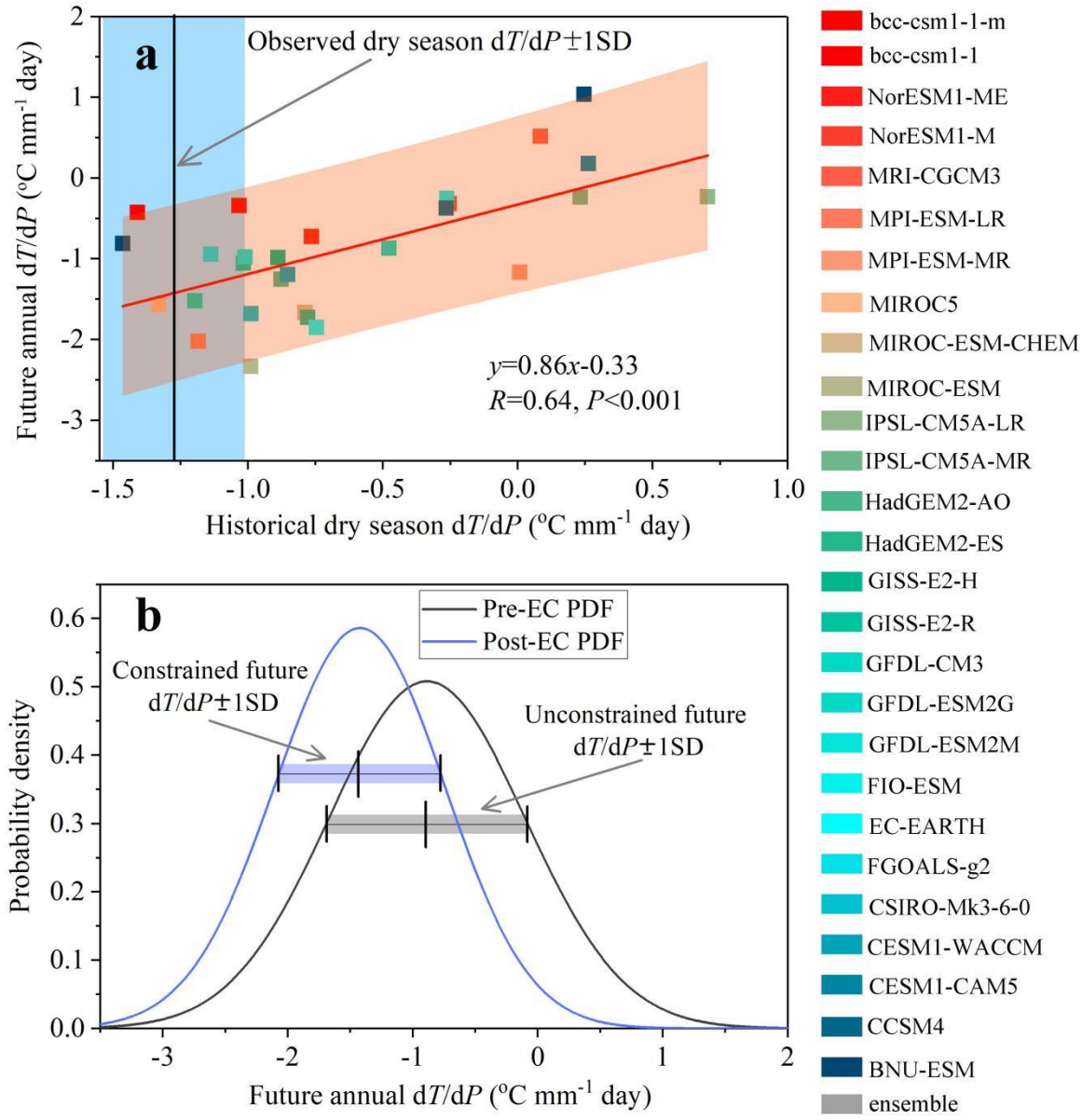

Supplementary Fig. 11 EC on future annual d*T*/d*P* based on CMIP5 models under the RCP2.6 scenario. a, The constraint consists of a linear regression (with the associated forecast error) between the future annual simulated d*T*/d*P* and historical simulated dry-season d*T*/d*P* (red line and orange shaded area); then the constrained data is computed by projecting the observed historical dry season d*T*/d*P* ± one standard deviation (vertical black line and light blue rectangle, obtained from the HadCRUT4 dataset) onto the regression. **b,** Blue and grey lines are PDFs for the constrained (post-EC) and unconstrained (Pre-EC) future annual d*T*/d*P*, showing the change in forecast uncertainty and the best estimate of future annual d*T*/d*P*.

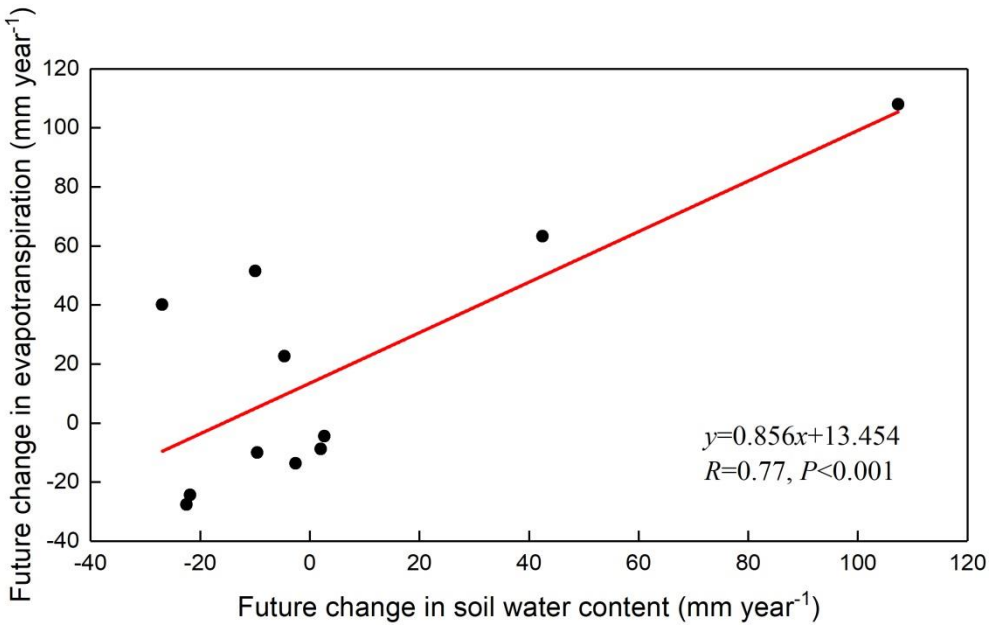

Supplementary Fig. 12 Linear regression between future changes in tropical soil water content and in tropical land evapotranspiration based on CMIP6 models (see Supplementary Table 1) for the SSP585 scenario.

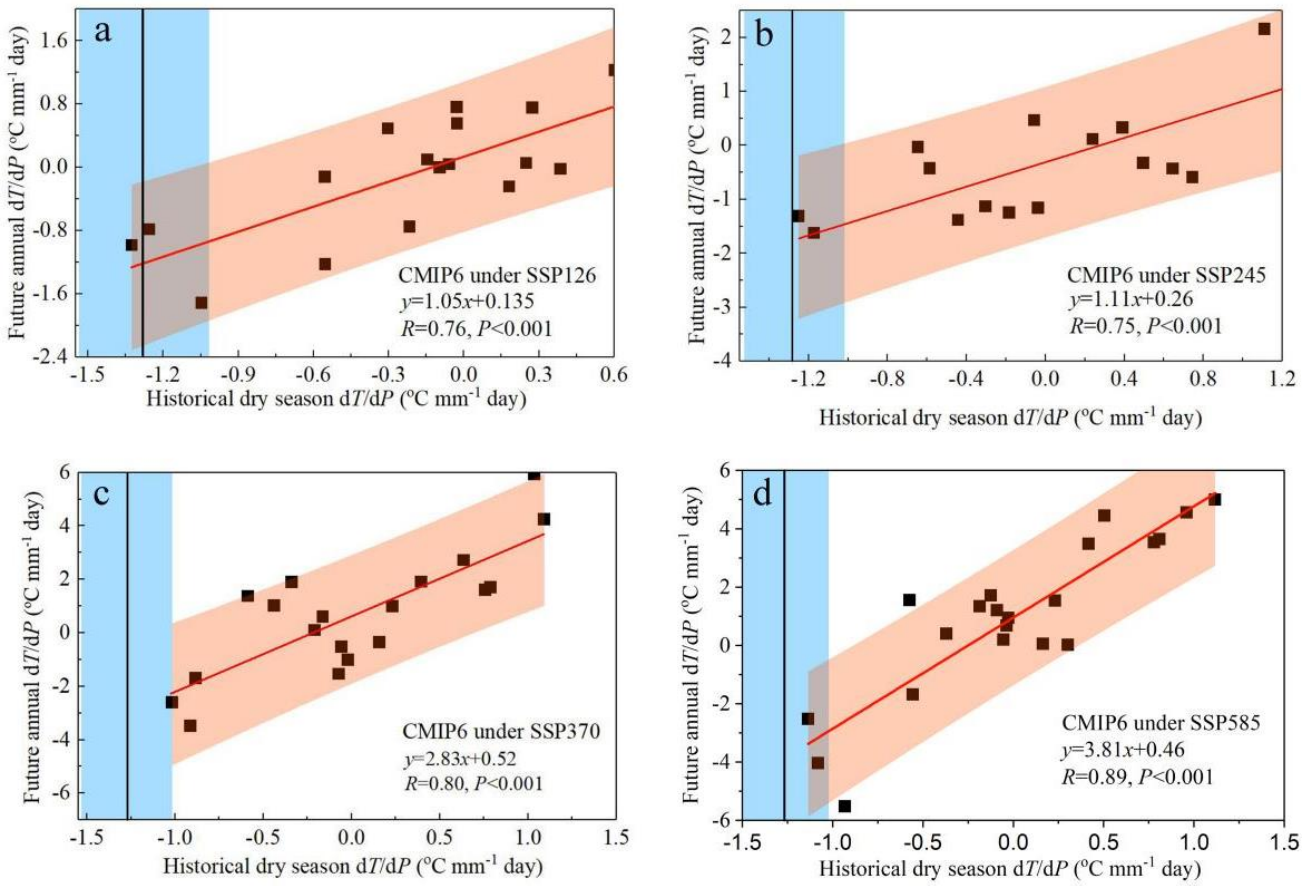

Supplementary Fig. 13 EC on future annual d*T*/d*P* based on CMIP6 models under SSP126 (a), SSP245 (b), SSP370 (c) and SSP585 (d) scenarios for the tropical land-surface area in which the subareas where dry-season months are not defined as May to July have been excluded.

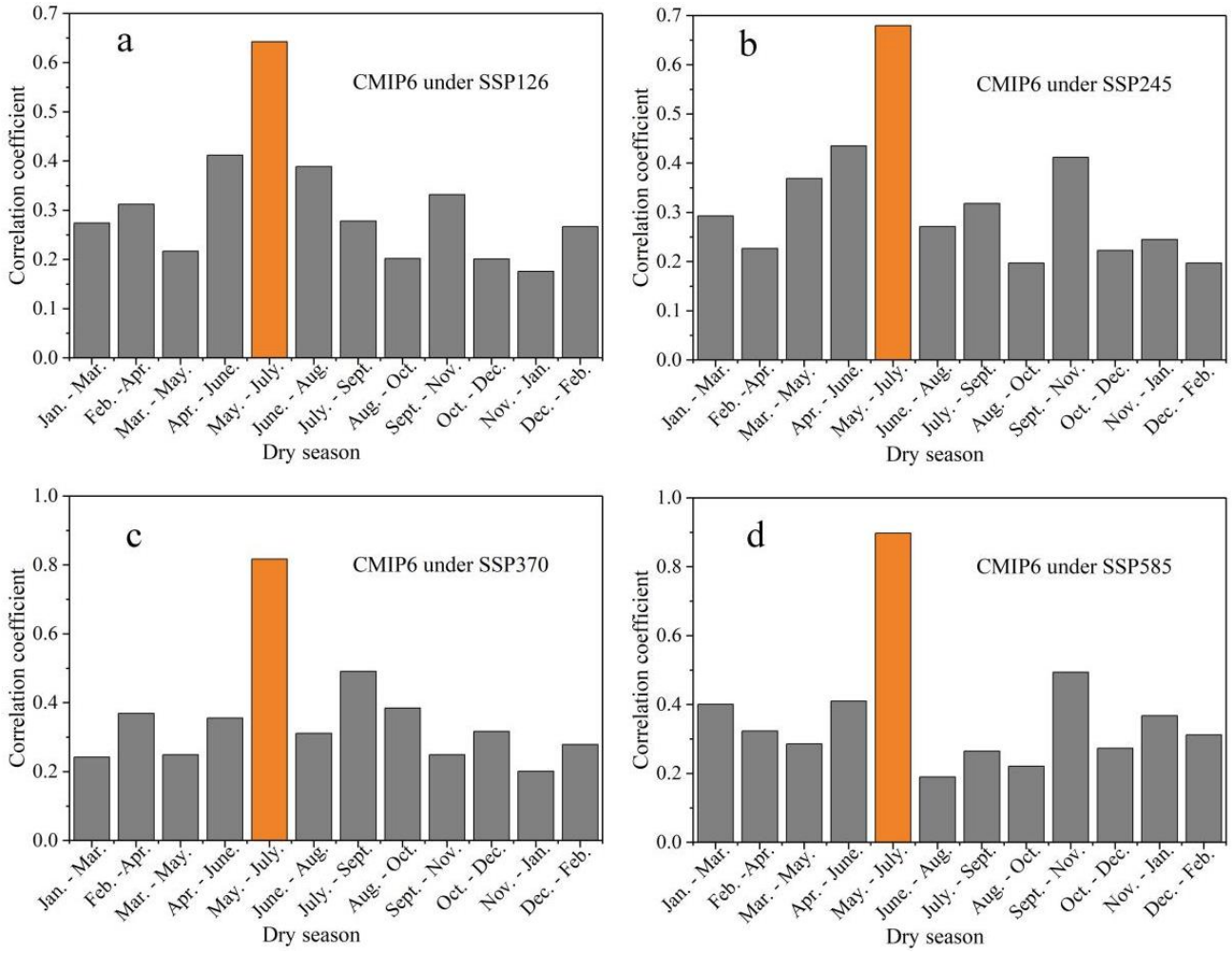

Supplementary Fig. 14 Correlation coefficients of emergent relationships between historical monthly d*T*/d*P* and future annual d*T*/d*P* based on CMIP6 models under SSP126 (a), SSP245 (b), SSP370 (c) and SSP585 (d) scenarios.

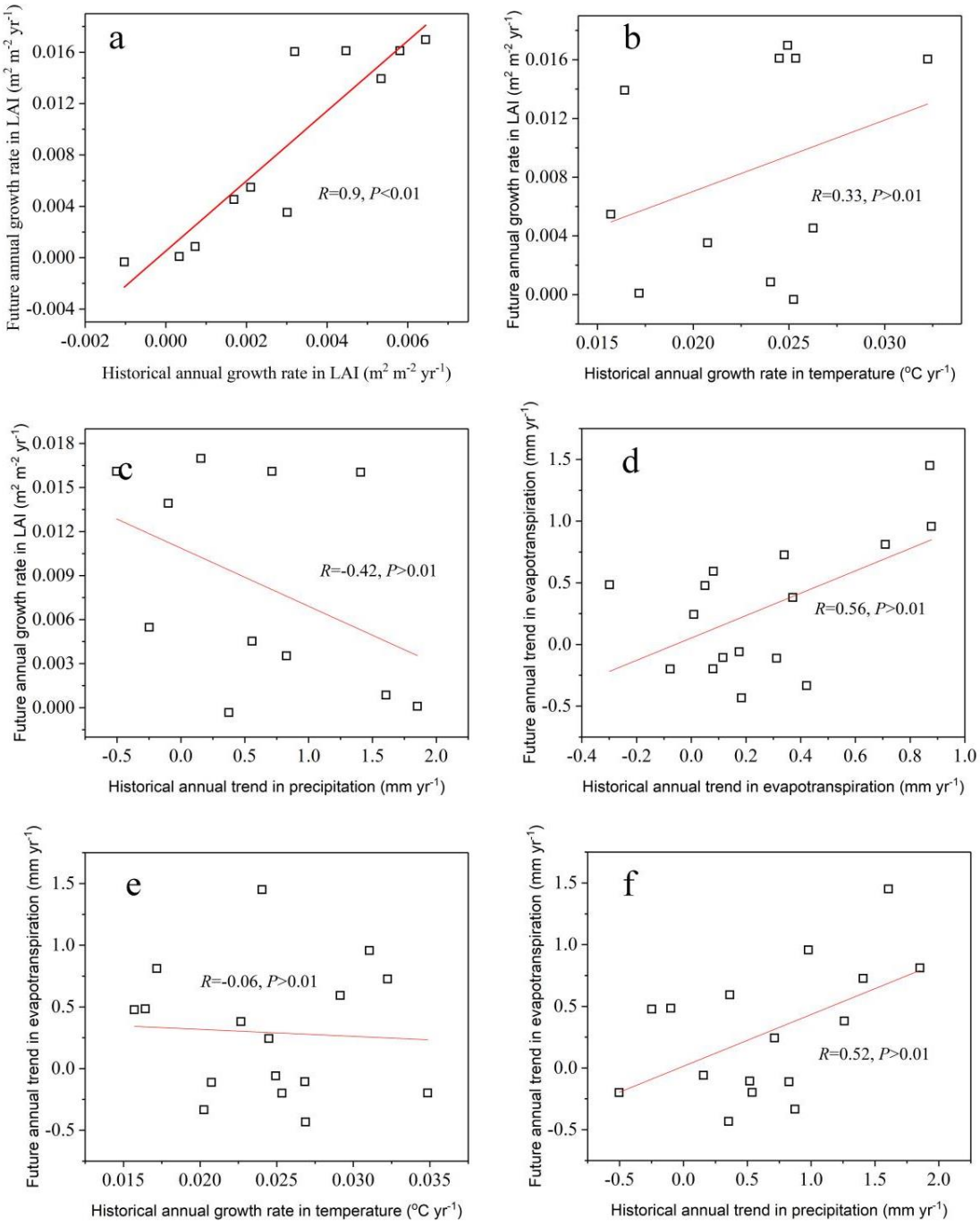

Supplementary Fig. 15 Other possible emergent constraints on tropical land evapotranspiration and LAI based on CMIP6 models. a, Emergent relationship between historical annual growth rate in LAI and future annual growth rate in LAI. **b,** Emergent relationship between historical annual growth rate in temperature and future annual growth rate in LAI. **c,** Emergent relationship between historical annual trend in precipitation and future annual growth rate in LAI. **d,** Emergent relationship between historical annual trend in evapotranspiration and future annual trend in evapotranspiration. **e,** Emergent relationship between historical annual growth rate in temperature and future annual trend in evapotranspiration. **f,** Emergent relationship between historical annual trend in precipitation and future annual trend in evapotranspiration. Note: There is a more significant relationship between historical LAI and future LAI than between historical *GPP* and future LAI, given that *GPP* provides a comprehensive measure of the photosynthesis, carbon sequestration and water use efficiency (and etc.) of a total regional phytocoenosium, and therefore we do not test *GPP* herein.

Supplementary Table 1 CMIP6 models employed in this study

Models for temperature/precipitationunder SSP126	Models for temperature/precipitation under SSP245	Models for temperature/precipitation under SSP370	Models for temperature/precipitation under SSP585	Models for evapotranspiration under SSP585	Models for leaf area index SSP585	Models for soil water SSP585
GFDL-ESM4	ACCESS-ESM1-5	GFDL-ESM4	GFDL-ESM4	ACCESS-ESM1-5	BCC-CSM2-MR	ACCESS-ESM1-5
CanESM5-CanOE	BCC-CSM2-MR	ACCESS-ESM1-5	ACCESS-ESM1-5	BCC-CSM2-MR	CanESM5-CanOE	BCC-CSM2-MR
ACCESS-ESM1-5	MIROC6	NorESM2-MM	NorESM2-MM	CanESM5-CanOE	CESM2	CanESM5-CanOE
NorESM2-MM	CNRM-CM6-1	MRI-ESM2-0	CESM2-WACCM	CESM2	CESM2-WACCM	CNRM-ESM2-1
BCC-CSM2-MR	GFDL-CM4	CNRM-ESM2-1	HadGEM3-GC31-LL	CESM2-WACCM	FIO-ESM-2-0	HadGEM3-GC31-LL
MCM-UA-1-0	NorESM2-MM	CESM2	UKESM1-0-LL	CNRM-ESM2-1	GFDL-CM4	INM-CM4-8
UKESM1-0-LL	FGOALS-f3-L	UKESM1-0-LL	CESM2	HadGEM3-GC31-LL	INM-CM4-8	INM-CM5-0
CESM2-WACCM	CanESM5-CanOE	BCC-CSM2-MR	MIROC6	INM-CM4-8	INM-CM5-0	MIROC6
MRI-ESM2-0	FIO-ESM-2-0	KACE-1-0-G	GFDL-CM4	INM-CM5-0	MIROC-ES2L	MRI-ESM2-0
CESM2	NorESM2-LM	MIROC6	CNRM-ESM2-1	KACE-1-0-G	MRI-ESM2-0	NorESM2-MM
HadGEM3-GC31-LL	CESM2-WACCM	MIROC-ES2L	CanESM5-CanOE	MCM-UA-1-0	NorESM2-MM	UKESM1-0-LL
KACE-1-0-G	MIROC-ES2L	CanESM5-CanOE	BCC-CSM2-MR	MIROC6		
CNRM-CM6-1	MCM-UA-1-0	FGOALS-f3-L	MRI-ESM2-0	MIROC-ES2L		
CNRM-ESM2-1	CESM2	MPI-ESM1-2-LR	MIROC-ES2L	MRI-ESM2-0		
CNRM-CM6-1-HR	INM-CM5-0	MCM-UA-1-0	KACE-1-0-G	NorESM2-MM		
MIROC6	INM-CM4-8	CNRM-CM6-1	FGOALS-f3-L	UKESM1-0-LL		
IPSL-CM6A-LR		ACCESS-CM2	MCM-UA-1-0			
		INM-CM5-0	ACCESS-CM2			
		INM-CM4-8	FIO-ESM-2-0			
			INM-CM4-8			
			INM-CM5-0			

Supplementary Table 2 Observed values for seasonal dT/dP ± one standard deviation from the four datasets and forecasted annual values based on CMIP6 models before and after EC use under the four SSP scenarios

Datasets	Observed dry season dT/dP ± one standard deviation (℃ mm^{-1} day)	SSP scenario	Pre-EC value of future annual dT/dP ± one standard deviation (℃ mm^{-1} day)	Post-EC value of future annual dT/dP ± one standard deviation (℃ mm^{-1} day)
HadCRUT4	-1.28 ± 0.26	SSP126	-0.14 ± 0.72	-1.10 ± 0.65
		SSP245	-0.27 ± 1.10	-1.63 ± 0.92
		SSP370	0.57 ± 2.24	-2.86 ± 1.58
		SSP585	1.03 ± 2.60	-3.52 ± 1.52
GISS+GPCC	-0.99 ± 0.26	SSP126	-0.14 ± 0.72	-0.82 ± 0.63
		SSP245	-0.27 ± 1.10	-1.32 ± 0.91
		SSP370	0.57 ± 2.24	-2.07 ± 1.53
		SSP585	1.03 ± 2.60	-2.46 ± 1.50
NOAA+GPCC	-0.97 ± 0.21	SSP126	-0.14 ± 0.72	-0.81 ± 0.61
		SSP245	-0.27 ± 1.10	-1.30 ± 0.90
		SSP370	0.57 ± 2.24	-2.03 ± 1.49
		SSP585	1.03 ± 2.60	-2.41 ± 1.41
Delaware	-1.37 ± 0.20	SSP126	-0.14 ± 0.72	-1.17 ± 0.65
		SSP245	-0.27 ± 1.10	-1.72 ± 0.92
		SSP370	0.57 ± 2.24	-3.08 ± 1.54
		SSP585	1.03 ± 2.60	-3.82 ± 1.42